

# Visualization of ferromagnetic domains in $\text{TbNi}_2\text{B}_2\text{C}$ and $\text{ErNi}_2\text{B}_2\text{C}$ single crystals: Weak ferromagnetism and its coexistence with superconductivity.

I.S. Veschunov, L.Ya. Vinnikov

*Institute of Solid State Physics RAS, Chernogolovka,  
Moscow region 142432, Russian Federation*

S.L. Bud'ko, P.C. Canfield

*Ames Laboratory US DOE and Department of Physics and Astronomy,  
Iowa State University, Ames, IA 50011, USA*

(Dated: October 30, 2018)

## Abstract

The magnetic flux structure in the basal plane, (001), of single crystals of superconducting ( $\text{R} = \text{Er}$ ) and non-superconducting ( $\text{R} = \text{Tb}$ )  $\text{RNi}_2\text{B}_2\text{C}$  was studied by high resolution Bitter decoration at temperatures below  $T_c$  (superconducting transition) and/or  $T_N$  (antiferromagnetic transition). For both materials two sets of domain boundaries, in  $\{110\}$  and  $\{100\}$  planes, were observed. The temperature ranges in which the  $\{100\}$  domain boundaries were observed in  $\text{TbNi}_2\text{B}_2\text{C}$  and  $\text{ErNi}_2\text{B}_2\text{C}$  coincide with the weak ferromagnetic (WFM) ordering in these materials. On the other hand, the  $\{110\}$  twin boundaries - the antiferromagnetic domain boundaries - were observed in both compounds below  $T_N$ . The possibility of interpretation of  $\{100\}$  boundaries as Bloch domain walls in the weakly ferromagnetic phase, for  $T < T_{WFM} < T_N$  ( $\text{TbNi}_2\text{B}_2\text{C}$ ) or  $T < T_{WFM} < T_N < T_c$  ( $\text{ErNi}_2\text{B}_2\text{C}$ ) is discussed.

PACS numbers: 75.50.Ee, 75.60.Ch

The coexistence of superconductivity and magnetism is studied in two distinct classes of materials: artificially structured (multilayered) systems<sup>1,2,3,4</sup> and spatially uniform (bulk) crystals. The coexistence of ferromagnetism and superconductivity in bulk materials has been observed in a very limited number of cases. In the  $\text{RRh}_4\text{B}_4$  series the temperature interval of coexistence of superconductivity and ferromagnetism is rather narrow<sup>5,6</sup>. For superconducting ferromagnets with  $T_c < T_{FM}$  (rutheno-cuprates, uranium compounds under pressure) a variety of domain structures has been predicted<sup>7,8</sup>. Over the past decade, the family of rare earth borocarbides,  $\text{RNi}_2\text{B}_2\text{C}$  ( $\text{R}$  = rare earth)<sup>9</sup> has become a convenient model system in which long range magnetic order (associated with magnetic rare earth ions<sup>10</sup>), superconductivity and the coexistence of these two phenomena is observed with the specific ground state depending on the specific rare earth ion<sup>11,12,13,14</sup>. For example, for  $\text{R} = \text{Y}, \text{Lu}$ , superconductivity with  $T_c \approx 15.5$  K and 16.5 K, respectively, was observed, while  $\text{GdNi}_2\text{B}_2\text{C}$  has an antiferromagnetic transition at  $T_N \approx 20$  K and no superconductivity (down to 30 mK). In  $\text{ErNi}_2\text{B}_2\text{C}$  superconductivity ( $T_c \approx 10.5$  K) coexists with magnetic long range order: antiferromagnetism, AFM, ( $T_N \approx 6$  K) and weak ferromagnetism, WFM, ( $T_{WFM} \approx 2.3$  K)<sup>15</sup>. It is important to mention that in the AFM and WFM phases the magnetic moment is confined to the basal plane, (001), with the easy axis along [100] or [010] direction<sup>16,17</sup>. For  $\text{TbNi}_2\text{B}_2\text{C}$  two magnetic phases, AFM ( $T_N \approx 15$  K) and WFM ( $T_{WFM} \approx 8$  K) were reported<sup>18,19</sup>.

The magnetic flux structures in  $\text{RNi}_2\text{B}_2\text{C}$  ( $\text{R} = \text{Er}, \text{Ho}, \text{Tb}$ ) single crystals (in a limited range of temperatures and magnetic fields) were recently studied by high resolution Bitter decoration technique<sup>20,21,22</sup>. For  $\text{ErNi}_2\text{B}_2\text{C}$  and  $\text{HoNi}_2\text{B}_2\text{C}$  antiferromagnetic domains induced by magnetoelastic interactions were observed<sup>20,22</sup>. In these materials, vortex pinning was detected on the  $\{110\}$  twin AFM domain boundaries in the orthorhombic phase. Unexpectedly, magnetic contrast on similar,  $\{110\}$  - type boundaries was also observed in non-superconducting  $\text{TbNi}_2\text{B}_2\text{C}$ <sup>21</sup>. The nature of this magnetic contrast remains unclear. Additionally, in some regions of the (001) surface, a more complex pattern was observed: in addition to the dominant stripes along  $\{110\}$  boundaries, a fine structure on [100] and [010] boundaries was observed (see Fig. 3c in Ref. 21).

In this work, to elucidate the nature of the domain structure associated with the AFM and WFM phases,  $\text{TbNi}_2\text{B}_2\text{C}$  and  $\text{ErNi}_2\text{B}_2\text{C}$  single crystals were studied by high resolution

Bitter decoration at temperatures that extend the lower limit of this technique. This is done so as to study the WFM phase of  $\text{ErNi}_2\text{B}_2\text{C}$  at  $T \sim T_{WFM} \approx 2.3$  K. These compounds are similar in their crystal structure and magnetic order, in particular they have a transition to WFM state below the respective Neel temperature, and therefore are suitable for a comparative study. We observed characteristic features of magnetic contrast in basal (001) plane along  $\langle 100 \rangle$  and  $\langle 110 \rangle$  directions in non-superconducting  $\text{TbNi}_2\text{B}_2\text{C}$  crystals. In addition, preferential accumulation of vortices in (100) and (010) planes, distinct from the pinning by  $\{110\}$  - type twin boundaries, were observed for the first time in superconducting  $\text{ErNi}_2\text{B}_2\text{C}$  single crystals just above  $T_{WFM} = 2.3$  K.

The Bitter decoration technique is based on the segregation of fine dispersed magnetic particles on the surface of a superconductor or a magnetic material due to the regions of inhomogeneous magnetic flux<sup>23,24</sup>. Scanning electron microscope images of the magnetic particle distribution (bright dots in the figures below) provide information about the structure of vortices or magnetic domains. The high resolution ( $< 100$  nm) of this technique is due to the small size of the magnetic particles ( $< 10$  nm) that are produced, at low temperature, by evaporation of the magnetic material (in our case, iron) from the surface of a tungsten wire in a buffer gas (helium) atmosphere at low pressure ( $\sim 10^{-2}$  Torr)<sup>24</sup>.

$\text{TbNi}_2\text{B}_2\text{C}$  and  $\text{ErNi}_2\text{B}_2\text{C}$  single crystals were grown using a  $\text{Ni}_2\text{B}$ , high temperature flux method<sup>11,25</sup>. As grown (001) surfaces with approximate dimensions of  $3 \times 5$  mm<sup>2</sup> were used in these experiments. The decoration was performed in the field-cooled regime with the magnetic field  $\sim 20$  Oe for  $\text{ErNi}_2\text{B}_2\text{C}$  and  $\sim 1.1$  kOe for  $\text{TbNi}_2\text{B}_2\text{C}$ , applied along the  $c$  axis of the crystals (this 50 - fold difference in applied field is associated with the fact that in  $\text{ErNi}_2\text{B}_2\text{C}$  the vortices provide the flux contrast whereas in  $\text{TbNi}_2\text{B}_2\text{C}$  the contrast has to come directly from the local moment structure).

The decoration temperature,  $T_d$ , was in the range of 2.6 K to 15 K. It should be mentioned that in these experiments the decoration temperature is defined as the temperature of the gas measured by a resistive thermometer, placed in the vicinity of the sample, just after the current through the evaporator is turned on. During the thermal evaporation of iron the heating of the system occurs so that the temperature in the evaporation chamber may increase by several degrees, therefore in the experiment the decoration chamber is initially cooled down to the temperature  $T_1$  ( $T_1 < T_d$ ). The decoration temperature,  $T_d$ , is minimized

by decrease of the size (mass) of the evaporator using a 0.05 mm diameter tungsten wire. The lowest  $T_d$  in decoration experiments reported in the literature so far is 2.9 K<sup>26</sup>. In our experiments the lowest temperature  $T_1$  was 1.6 K, in this case the  $T_d$  was estimated as 2.6 K. These reduced temperatures allow us to try to image the WFM state in  $\text{ErNi}_2\text{B}_2\text{C}$  which has  $T_1 < (T_{WFM} \approx 2.3 \text{ K}) \leq T_d$ .

Scanning electron microscope (SEM) was used for visualization of the decoration patterns after warming of the sample up to the room temperature.

A Bitter decoration pattern on the (001) surface of  $\text{TbNi}_2\text{B}_2\text{C}$  single crystal after field cooling in a field of  $H = 1.1 \text{ kOe}$  applied along the  $c$  axis is shown in Fig. 1. One type of domain boundaries are aligned along the  $\langle 110 \rangle$  directions. These are often separated by 3-10  $\mu\text{m}$ , but (as can be seen in Fig. 1) can also have much larger spacings as well. A second set of boundaries, aligned along the  $\langle 100 \rangle$  directions appear with an order of magnitude smaller separation between them. Similar structures were observed in  $\text{TbNi}_2\text{B}_2\text{C}$  for temperatures  $T_d$  below 8 K. Graphically similar patterns (regions with two distinct sets of boundaries) were observed in other parts of the sample and in different samples. A detailed discussion of the magnetic flux structures observed in  $\text{TbNi}_2\text{B}_2\text{C}$  single crystals in a wide range of temperatures and magnetic fields will be presented elsewhere<sup>27</sup>.

The symmetry of the  $\text{TbNi}_2\text{B}_2\text{C}$  crystal structure allows for formation of AFM structures with a weak ferromagnetic component in the basal,  $(ab)$  plane<sup>18,19</sup>. The direction of the weak ferromagnetic moment coincides with the direction of the longitudinally polarized spin density wave along  $[100]$  or  $[010]$ . The temperature range in which the fine structure in decoration patterns is observed along these directions coincides with the temperatures at which WFM phase is observed in  $\text{TbNi}_2\text{B}_2\text{C}$ . It is natural then to suppose that the observed fine structure corresponds to the boundaries of the WFM domains, i.e. these boundaries cause the appearance of the magnetic contrast. Since the Bitter decoration technique is only sensitive to the component of the inhomogeneous magnetic field perpendicular to the surface, the observed domain boundaries are most probably of the Bloch type. It is possible that the boundaries between the AFM domains with mutually perpendicular directions of the spin density wave contribute to the magnetic contrast as well<sup>21</sup>.

For this work it is important to note that  $\text{TbNi}_2\text{B}_2\text{C}$  is magnetically similar to  $\text{ErNi}_2\text{B}_2\text{C}$ : similar local moment anisotropy and similar antiferromagnetic order that leads to similar

weak ferromagnetism at lower temperatures. The key differences between  $\text{ErNi}_2\text{B}_2\text{C}$  and  $\text{TbNi}_2\text{B}_2\text{C}$  are that  $T_N$  and  $T_{WFM}$  for  $\text{ErNi}_2\text{B}_2\text{C}$  are substantially lower than those for  $\text{TbNi}_2\text{B}_2\text{C}$  and  $\text{ErNi}_2\text{B}_2\text{C}$  superconducts below  $T_c \approx 10.5$  K. This means that in  $\text{ErNi}_2\text{B}_2\text{C}$  the interaction of vortices with magnetic order can be probed. In particular, if the base temperature for decoration,  $T_1$ , is below  $T_{WFM} = 2.3$  K and the decoration temperature,  $T_d$ , only slightly exceeds  $T_{WFM}$ , then in addition to vortices pinned along the AFM domain boundaries in the  $\{110\}$  planes,<sup>20,22</sup> other features may be observed. Indeed, rows of vortices along the  $\langle 100 \rangle$  directions were detected in several regions (where the twin boundaries were absent) of the  $\text{ErNi}_2\text{B}_2\text{C}$  crystal (Fig. 2). A Fourier transform of this pattern (shown in the inset to Fig. 2) confirms the alignment of the rows of vortices along  $[010]$  (seen as a line in  $[100]$  direction in the insert) and allows for the estimate of the minimum distance between the rows of vortices to be of the order of several hundreds nanometers.

Although the data presented in figure 2 are compelling it does have to be pointed out that these data have been collected at the edge of what the Bitter decoration technique can achieve. It should again be noted that whereas  $T_1$  is below  $T_{WFM}$ ,  $T_d$  is above this key temperature. This makes the decoration a dynamic process: e.g. one that takes place as the sample is warming toward  $T_{WFM}$  from below. In addition the data have been collected at the edge of what the  $\text{ErNi}_2\text{B}_2\text{C}$  samples allow in terms of resolvability and reproducibility. The pinning of the vortices along the  $\langle 100 \rangle$  directions is only clearly seen in regions of the sample where the  $\{110\}$  twin boundaries are absent. The details of the twin boundary spacing appear to be sample dependent and are probably are complex functions of multiple extrinsic, strain effects.

In order to (i) more fully detail the effects of WFM on vortex state and (ii) illustrate the difficulty of these experiments, a further set of experiments followed the evolution of the patterns observed on the same region of the (001) surface of a  $\text{ErNi}_2\text{B}_2\text{C}$  crystal that was cooled down to different temperatures: (a)  $T_1 < T_{WFM}$  and (b)  $T_{WFM} < T_1 < T_N$  before decoration. The protocol of the experiments is shown schematically in Fig. 3. Two distinct scenarios were observed. In the first case (scenario I) after the crystal was cooled down to  $T_1 < T_{WFM} \approx 2.3$  K<sup>16,17</sup> and decorated at  $T_d \geq T_{WFM}$  rows of vortices along  $[100]$  were observed, Fig. 4a. These rows could be easily seen on the left side of the pattern. The second image (Fig. 4b) shows a decoration pattern of the same single crystal (after the magnetic particles from the first decoration were carefully removed) obtained in different conditions:

the crystal was cooled down to  $T_1 = 4.2 \text{ K} > T_{WFM}$  and decoration temperature was  $T_d = 5.5 \text{ K} < T_N \approx 6 \text{ K}$ . The left side of the image (where no  $\langle 110 \rangle$  twin boundaries are present) shows triangular vortex lattice without a preferential orientation of the close-packed directions of the lattice along  $[100]$ . The patterns shown in Figs. 4a,b are reproducible on subsequent decoration experiments after cycling of the sample to room temperature.

In the second case (scenario II), in decoration experiments on a different  $\text{ErNi}_2\text{B}_2\text{C}$  crystal, the first cooling down to  $T_1 < T_{WFM}$  and decoration at  $T_d \geq T_{WFM}$  resulted in the pattern shown in Fig. 5a, with rows of vortices along  $\langle 100 \rangle$  directions observed in several parts of the crystal where the twin boundaries along  $\{110\}$  were absent. On a subsequent cooling down to  $T_1 = 4.2 \text{ K} > T_{WFM}$  and decoration below  $T_N$  only rows of vortices along twin boundaries  $\{110\}$  were observed, including the regions of the crystal where they were absent on initial decoration experiment (Fig. 5b). It is important to mention that only patterns similar to one in Fig. 5b were observed in further experiments on this crystal.

Out of six  $\text{ErNi}_2\text{B}_2\text{C}$  crystals studied, scenario I was realized in two, scenario II was observed in one, and the other three crystals showed only the  $\{110\}$  twin boundaries.

In all cases they were observed, the distance between the rows of vortices along the  $\langle 100 \rangle$  direction in  $\text{ErNi}_2\text{B}_2\text{C}$  is much smaller than between the rows of vortices along the  $\langle 110 \rangle$  (Figs. 2,4,5), similar to the distances between alleged magnetic domain boundaries in  $\text{TbNi}_2\text{B}_2\text{C}$  crystals (Fig. 1).

Our observations in  $\text{ErNi}_2\text{B}_2\text{C}$  crystals can be interpreted as a visualization of the pinning of vortices on the WFM domains boundaries in  $(100)$  or  $(010)$  planes. Since we did not succeed in lowering  $T_d$  for  $\text{ErNi}_2\text{B}_2\text{C}$  crystals below  $T_{WFM} = 2.3 \text{ K}$ , we possibly observe the remnant pinning of vortices at  $T_d$  slightly above  $T_{WFM}$  that does not vanish due to kinetics reasons. It is plausible that the vortices forming the rows "freeze" at the domain boundaries of the low temperature WFM phase, thus visualizing the domain boundaries in the  $(100)$  or  $(010)$  planes. The distance between the rows of vortices is probably not exactly the distance  $l$  between the WFM domain boundaries due to the repulsive interaction between vortices that exists even in small ( $< 100 \text{ Oe}$ ) magnetic fields. From Figs. 2,4,5 the reasonable estimate of  $l$  seems to be  $l < 1 \mu\text{m}$ . The width of the domain wall,  $w$ , and the width of the domain,  $l$  can be estimated following the theoretical model<sup>7</sup> for domain structure in superconducting ferromagnets: if such magnetic domains exist, the width of the domain wall should be less

than superconducting penetration depth,  $\lambda$ . If we take the size of the AFM domain,  $d$ , as an effective size of the region of the AFM to WFM transformation, and use the condition  $w \leq \lambda$ , then  $l \approx \sqrt{dw}$ . For  $\text{ErNi}_2\text{B}_2\text{C}$ , using  $\lambda = 70 \text{ nm}^{28}$  and  $d \approx 7 \mu\text{m}$ ,  $l$  is estimated as  $\approx 700 \text{ nm}$ , similar to the observed distances between the rows of vortices along  $\langle 100 \rangle$  (Figs. 2,4,5). It should be stressed that although in both the  $\text{ErNi}_2\text{B}_2\text{C}$  and  $\text{TbNi}_2\text{B}_2\text{C}$  cases we are able to visualize WFM domain boundaries, in  $\text{TbNi}_2\text{B}_2\text{C}$  the magnetic particles image directly the magnetic flux gradients on the domain boundaries, whereas in  $\text{ErNi}_2\text{B}_2\text{C}$  we use magnetic flux gradient of superconducting vortices that interact with the magnetic domain boundaries as well as with each other. Thus the "texture" of the images pertaining to  $\text{ErNi}_2\text{B}_2\text{C}$  and  $\text{TbNi}_2\text{B}_2\text{C}$  is different.

AFM to WFM transition in  $\text{TbNi}_2\text{B}_2\text{C}$  and  $\text{ErNi}_2\text{B}_2\text{C}$  was discussed as a lock-in phase transformation from incommensurate to commensurate spin density wave<sup>29</sup>. Neutron scattering data<sup>29</sup> suggest that the domain size in WFM phase of  $\text{ErNi}_2\text{B}_2\text{C}$  is of the order of  $1000a$ , where  $a \approx 0.35 \text{ nm}$  is the lattice parameter of  $\text{ErNi}_2\text{B}_2\text{C}$ . This yields an estimate value  $l \approx 350 \text{ nm}$ , that is in a reasonable agreement with our results. Additionally, recently<sup>30</sup> the characteristic dimensions of the AFM domain structure in orthorhombic phase of  $\text{ErNi}_2\text{B}_2\text{C}$ , similar to  $\text{YBa}_2\text{Cu}_3\text{O}_7$  were estimated considering minimum of the elastic energy (WFM phase was not considered), the results are consistent with the picture presented here.

There were several attempts<sup>28,31</sup> to observe spontaneous flux line lattice in the WFM phase ( $T < T_{WFM} < T_c$ ) of  $\text{ErNi}_2\text{B}_2\text{C}$ . In neutron experiments<sup>31</sup> no spontaneous flux line lattice was observed in zero field cooled protocol, however a vortex phase was observed after magnetic field was applied below  $T_{WFM}$ , that is consistent with our observations that changes in decoration patterns were observed only if the sample was cooled in an applied field below  $T_{WFM}$ . Hall microscope measurements<sup>28</sup> were not able to resolve the structure of magnetic flux on (100) or (010) planes. An estimate of the spontaneous magnetization in the basal plane give the value of the in-plane magnetic induction  $\sim 700 \text{ G}$ , that corresponds to the period of  $\sim 0.16 \mu\text{m}$ , below the resolution of the Hall microscope<sup>28</sup>, for the anticipated spontaneous flux line lattice in (100) or (010) planes.

*In summary*, we observed (a) residual pinning of vortices on (100) or (010) boundaries in  $\text{ErNi}_2\text{B}_2\text{C}$  slightly above  $T_{WFM} = 2.3 \text{ K}$  that visualize the WFM domains in this material;

(b) magnetic contrast on (100) or (010) boundaries (that possibly are Bloch domain walls) in WFM phase of  $\text{TbNi}_2\text{B}_2\text{C}$ , below  $T_{WFM} = 8$  K.

The correspondence of the temperature intervals in which particular features in magnetic flux structure in  $\text{TbNi}_2\text{B}_2\text{C}$  and  $\text{ErNi}_2\text{B}_2\text{C}$  were observed with the (respective) temperature ranges of WFM ordering, as well as the orientation of these features with respect to crystallographic axis of the crystals give, in our opinion, strong support to our interpretation of the low temperature features in decoration patterns. However, the structure of domain walls and the nature of the magnetic contrast at  $\{110\}$  AFM domains in  $\text{TbNi}_2\text{B}_2\text{C}$  as well as possibility of formation and visualization of spontaneous flux line lattice in the WFM phase of  $\text{ErNi}_2\text{B}_2\text{C}$  remain as open problems and require further studies.

### Acknowledgments

The authors thank D.V. Matveyev for his assistance in SEM observations and G.V. Strukov for help in preparation of evaporators. This work was performed within the framework of the program of fundamental research "Effect of atomic, crystalline and electronic structures on properties of condensed matter" of the Division of Physical Sciences, Russian Academy of Sciences and Project RFFI-06-02-72025. Work at Ames Laboratory was supported by the US Department of Energy - Basic Energy Sciences under Contract No. DE-AC02-07CH11358.

- 
- <sup>1</sup> I.F. Lyuksyutov, V.L. Pokrovsky, Adv. Phys. **54**, 67 (2005).  
<sup>2</sup> A.I. Buzdin, Rev. Mod. Phys. **77**, 935 (2005).  
<sup>3</sup> V.V. Ryazanov, V.A. Oboznov, A.S. Prokof'ev, S.V. Dubonos, Pis'ma Zh. Exp. Teor. Fiz. **77**, 43 (2003) [JETP Lett. **77**, 39 (2003)].  
<sup>4</sup> V.V. Ryazanov, V.A. Oboznov, A.Yu. Rusanov, A.V. Veretennikov, A.A. Golubov, J. Aarts, Phys. Rev. Lett. **86**, 2427 (2001).  
<sup>5</sup> A.I. Buzdin, L.N. Bulaevskii, M.L. Kulić, S.V. Panyukov, Usp. Fiz. Nauk **144**, 597 (1984) [Sov. Phys. Uspekhi **27**, 927 (1984)].  
<sup>6</sup> Ø. Fischer, in: *Ferromagnetic Materials*, vol. 5, Eds. K.H.J. Buschow, E.P. Wohlfarth (Elsevier



- Science, Amsterdam, 1990) p. 465.
- <sup>7</sup> M. Faure, A.I. Buzdin, Phys. Rev. Lett. **94**, 187202 (2005).
  - <sup>8</sup> E.B. Sonin, Phys. Rev. B **66**, 100504 (2002).
  - <sup>9</sup> R.J. Cava, H. Takagi, B. Batlogg, H.W. Zandbergen, J.J. Krajewski, W.F. Peck Jr, R.B. van Dover, R.J. Felder, T. Siegrist, K. Mizuhashi, J.O. Lee, H. Eisaki, S. A. Carter, S. Uchida, Nature **367**, 146 (1994).
  - <sup>10</sup> J.W. Lynn, S. Skanthakumar, Q. Huang, S.K. Sinha, Z. Hossain, L.C. Gupta, R. Nagarajan, and C. Godart, Phys. Rev. B **55**, 6584 (1997).
  - <sup>11</sup> P.C. Canfield, P.L. Gammel, and D.J. Bishop, Phys. Today **51**(10), 40 (1998).
  - <sup>12</sup> K.-H. Müller, and V.N. Narozhnyi, Rep. Progr. Phys. **64** 943 (2001).
  - <sup>13</sup> K.-H. Müller, G. Fuchs, S.-L. Drechsler, and V.N. Narozhnyi, in: *Handbook of Magnetic Materials* vol. 14, Editor: K.H.J. Buschow (North-Holland, Amsterdam 2002) p. 199.
  - <sup>14</sup> S.L. Bud'ko and P.C. Canfield, Comptes Rendus Physique **7** 56 (2006).
  - <sup>15</sup> P.C. Canfield, S.L. Bud'ko, and B.K. Cho, Physica C **262**, 249 (1996).
  - <sup>16</sup> S.M. Choi, J.W. Lynn, D. Lopez, P.L. Gammel, P.C. Canfield, and S.L. Bud'ko, Phys. Rev. Lett. **87**, 107001 (2001).
  - <sup>17</sup> H. Kawano-Furukawa, H. Takeshita, M. Ochiai, T. Nagata, H. Yoshizawa, N. Furukawa, H. Takeya, and K. Kadowaki, Phys. Rev. B **65**, 180508 (2002).
  - <sup>18</sup> B.K. Cho, P.C. Canfield, and D.C. Johnston, Phys. Rev. B **53**, 8499 (1996).
  - <sup>19</sup> P. Dervenis, J. Zarestky, C. Stassis, A.I. Goldman, P.C. Canfield, and B.K. Cho, Phys. Rev. B **53**, 8506 (1996).
  - <sup>20</sup> N. Saha, R. Surdeanu, M. Marchevsky, G.J. Nieuwenhuys, C.D. Dewhurst, R.J. Wijngaarden, D.McK. Paul, and P.H. Kes, Phys. Rev. B **63**, 020502 (2000).
  - <sup>21</sup> L.Ya. Vinnikov, J. Anderegg, S.L. Bud'ko, P.C. Canfield, and V.G. Kogan, Pis'ma Zh. Eksp. Teor. Fiz. **77**, 600 (2003) [JETP Lett. **77**, 502 (2003)].
  - <sup>22</sup> L.Ya. Vinnikov, J. Anderegg, S.L. Bud'ko, P.C. Canfield, and V.G. Kogan, Phys. Rev. B **71**, 224513 (2005).
  - <sup>23</sup> H. Träube, U. Essmann, Phys. Status Solidi **18**, 813 (1966).
  - <sup>24</sup> L.Ya. Vinnikov, I.V. Grigor'eva, L.A. Gurevich, in: *The Real structure of High- $T_c$  Superconductors*, Springer Series in Materials Science, vol. 23, Ed. V.Sh. Shekhtman (Springer-Verlag, Berlin, Heidelberg, 1993) p. 89.

- <sup>25</sup> M. Xu, P.C. Canfield, J.E. Ostenson, D.K. Finnemore, B.K. Cho, Z.R. Wang, and D.C. Johnston, *Physica C* **227**, 321 (1994).
- <sup>26</sup> M.V. Marchevsky, Ph.D. Thesis, Leiden University (1997).
- <sup>27</sup> I.S. Veschunov, L.Ya. Vinnikov, S.L. Bud'ko, and P.C. Canfield, unpublished.
- <sup>28</sup> H. Bluhm, S.E. Sebastian, J.W. Guikema, I.R. Fisher, K.A. Moler, *Phys. Rev. B* **73**, 014514 (2006).
- <sup>29</sup> M.B. Walker, C. Detlefs, *Phys. Rev. B* **67**, 132407 (2003).
- <sup>30</sup> E.A. Brener, V.I. Marchenko, *Phys. Rev. Lett.* **97**, 067204 (2006).
- <sup>31</sup> H. Kawano-Furukawa, E. Habuta, T. Nagata, M. Nagao, H. Yoshizawa, N. Furukawa, H. Takeya, K. Kadowaki, preprint: cond-mat/0106273.

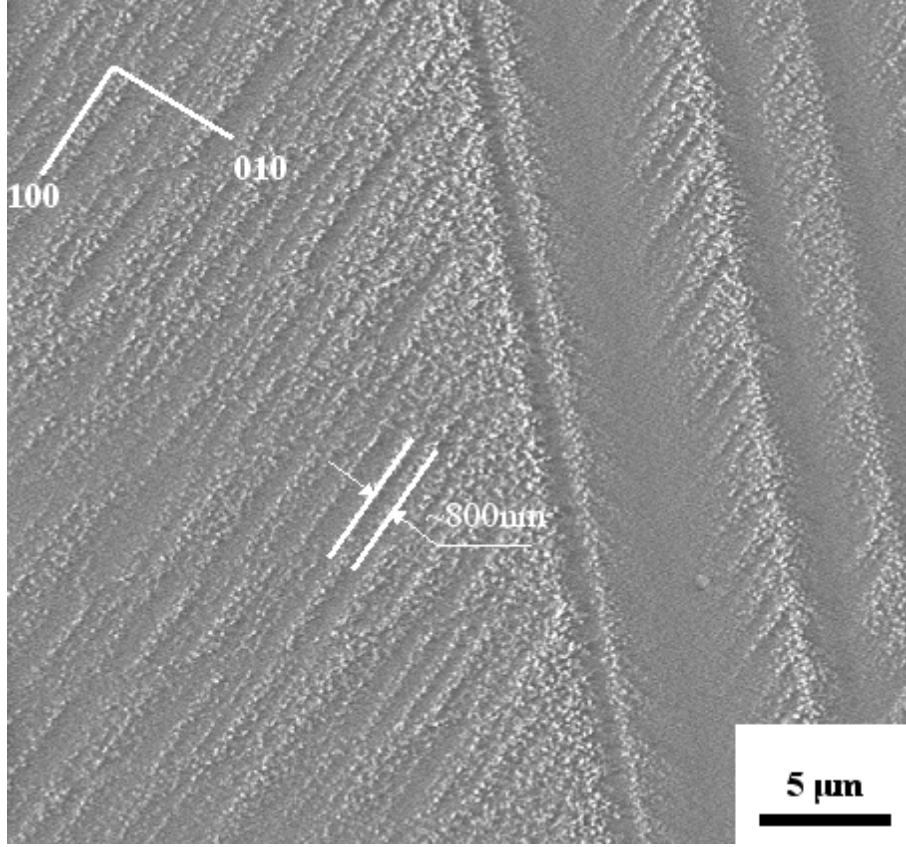


FIG. 1: Bitter decoration pattern on a TbNi<sub>2</sub>B<sub>2</sub>C single crystal cooled down to  $T_1 = 4.2$  K in a magnetic field of  $H = 1.1$  kOe and decorated at  $T_d \approx 7$  K.

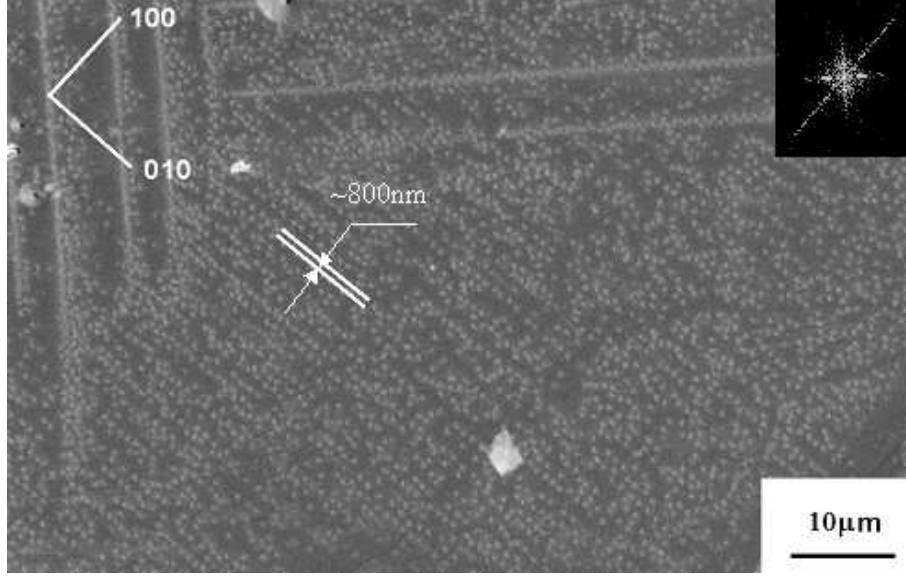


FIG. 2: Bitter decoration pattern on a twin-boundaries-free region of a  $\text{ErNi}_2\text{B}_2\text{C}$  single crystal cooled down to  $T_1 = 1.8$  K in a magnetic field of  $H = 20$  Oe and decorated at  $T_d \approx 4$  K. Inset: Fourier transform of the image.

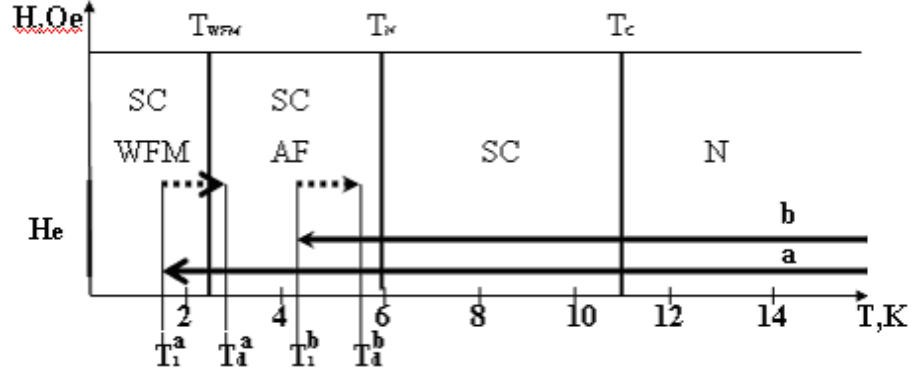


FIG. 3: Illustration of the protocols used in the low temperature experiment. Path (a): cooling down to  $T_1$  below  $T_{WFM}$ ,  $T_d$  slightly above  $T_{WFM}$ ; path (b): both  $T_1$  and  $T_d$  above  $T_{WFM}$  but below  $T_N$ .

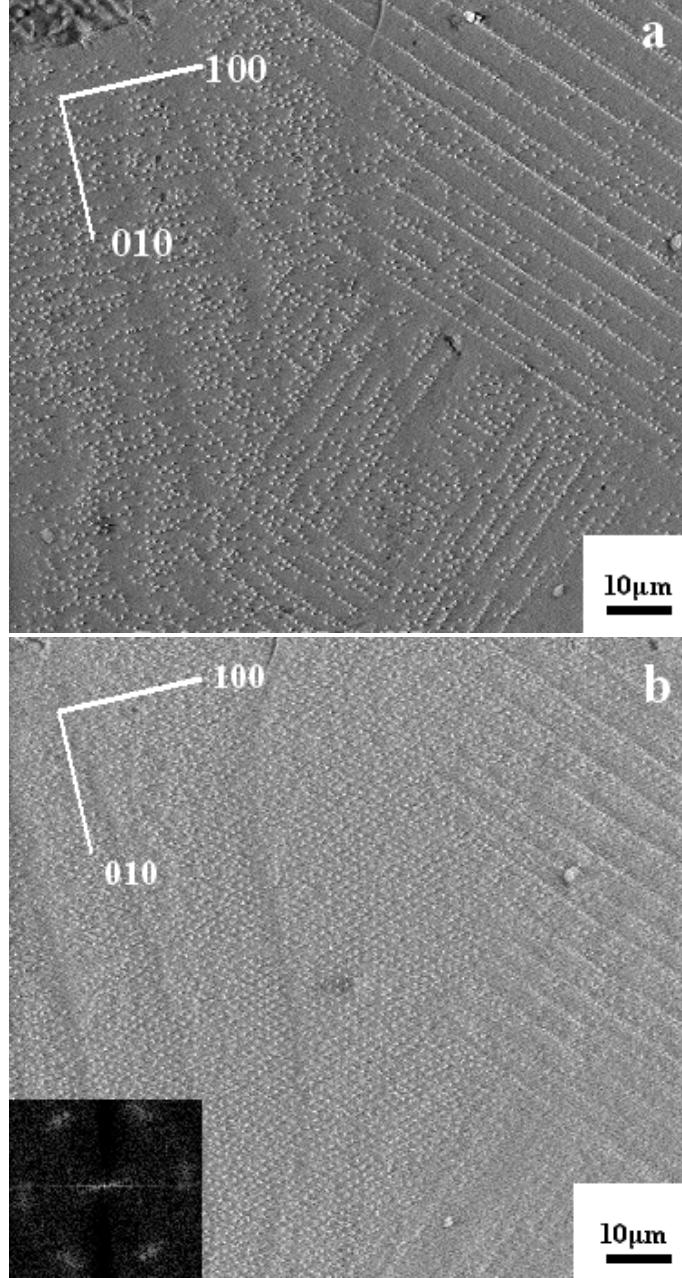


FIG. 4: Bitter decoration pattern on an  $\text{ErNi}_2\text{B}_2\text{C}$  single crystal (sample I) obtained after field cooling in an applied field  $H$ , using experimental protocols (a):  $T_1 = 1.8$  K,  $T_d = 2.6$  K,  $H = 15$  Oe (panel (a)) and (b):  $T_1 = 4.2$  K,  $T_d = 5.5$  K,  $H = 20$  Oe (panel b). Inset to panel (b): Fourier transform of the image from the left side of the pattern showing hexagonal order of vortices.

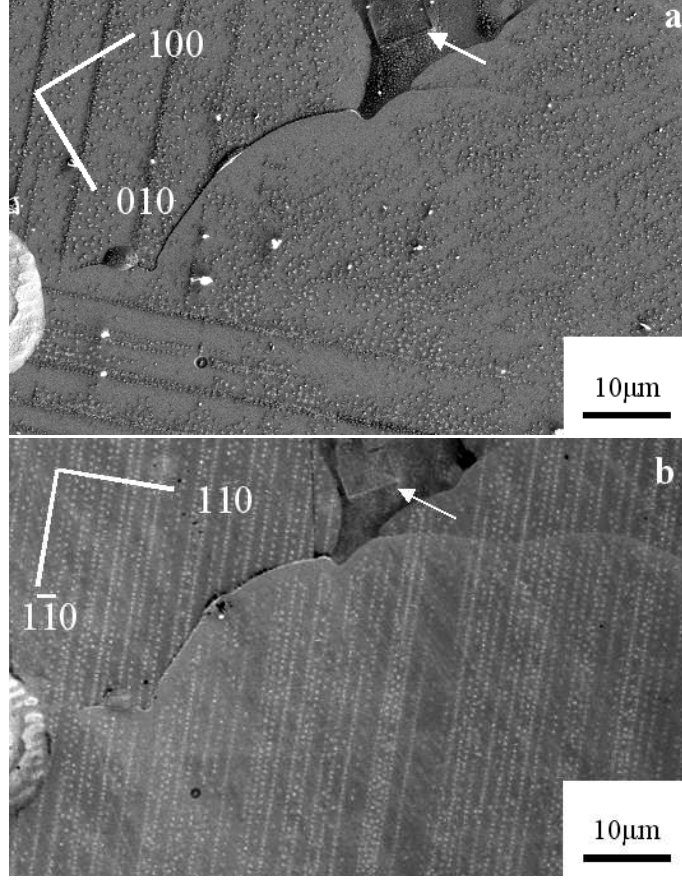


FIG. 5: Bitter decoration pattern on an  $\text{ErNi}_2\text{B}_2\text{C}$  single crystal (sample II) obtained after field cooling in applied field  $H$ , using experimental protocols (a):  $T_1 = 1.6$  K,  $T_d = 4.2$  K,  $H = 20$  Oe (panel (a)) and (b):  $T_1 = 4.2$  K,  $T_d = 5.5$  K,  $H = 20$  Oe (panel b).